

10/20/95 JSJ

Minimum Wakefield Achievable by Waveguide Damped Cavity*

Xintian E. Lin and Norman M. Kroll,
Stanford Linear Accelerator Center, Stanford University, Stanford, CA 94309
and University of California, San Diego, La Jolla, CA 92093

Abstract

We use an equivalent circuit to model a waveguide damped cavity. Both exponentially damped and persistent[1] (decay $t^{-3/2}$) components of the wakefield are derived from this model. The result shows that for a cavity with resonant frequency a fixed interval above waveguide cutoff, the persistent wakefield amplitude is inversely proportional to the external Q value of the damped mode. The competition of the two terms results in an optimal Q value, which gives a minimum wakefield as a function of the distance behind the source particle. The minimum wakefield increases when the resonant frequency approaches the waveguide cutoff. The results agree very well with computer simulation on a real cavity-waveguide system.

I. Introduction

Waveguide damping as a means to limit beam emittance growth due to the long range wakefield has received extensive study. The effectiveness of this procedure has typically been assessed by evaluating the resultant Q_{ext} of higher order cavity modes, thereby determining their exponential damping rate. Kroll and Lin[1] have pointed out another type of wakefield (persistent wakefield) associated with waveguide damping, which decays as $t^{-3/2}$.

We use an equivalent circuit model of a single mode cavity with waveguide damping to obtain an expression for the amplitude coefficient of the persistent term relative to that of the exponentially damped term. This expression is proportional to $\frac{1}{Q}$ with a coefficient which depends only upon the resonant and cutoff frequencies. It shows that the total wakefield at a fixed time delay is minimized by an optimum rather than minimum Q value.

II. Circuit Model

The circuit model is shown in Fig. 1. L_1 and C_1 form a

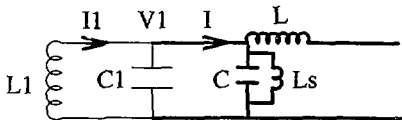


Figure 1. Thick line represents a transmission line. L , C , L_s are understood as distributed quantities.

lossless resonant circuit to mimic the cavity. The transmis-

sion line with shunt inductance L_s mimics the waveguide. We note that while L and C are inductance and capacitance per unit length, respectively, L_s is inductance times unit length.

A. Transmission Line with Shunt Inductance

The differential equations of the transmission line with shunt inductance are

$$\frac{\partial V}{\partial x} = -L \frac{\partial I}{\partial t} \quad \text{and} \quad (1)$$

$$\frac{\partial I}{\partial x \partial t} = -C \frac{\partial^2 V}{\partial t^2} - \frac{V}{L_s}. \quad (2)$$

Combining Eqs. 1 with 2, we obtain a single equation

$$LC \frac{\partial^2 V}{\partial t^2} - \frac{\partial^2 V}{\partial x^2} + \frac{L}{L_s} V = 0 \quad (3)$$

involving V only.

For a periodic ($e^{-i\omega t}$) field, the solutions are $V \sim e^{\pm ikx}$, with $k = \sqrt{LC} \sqrt{\omega^2 - \frac{1}{L_s L}}$. From Eq. 1, the voltage and current of the transmission line mode must be related by

$$\frac{V}{I} = \frac{\omega L}{\pm k} = \pm \sqrt{L} \frac{\omega}{\sqrt{\omega^2 - \omega_c^2}} \equiv Z, \quad (4)$$

where the \pm sign depends on the direction of the propagating waves: plus for positive x direction, negative for the other, and $\omega_c^2 = \frac{1}{L_s L}$.

B. Resonator with Transmission Line Loading

The differential equation of the voltage V_1 and current I_1 of the cavity follows the familiar equations of capacitance and inductance:

$$\frac{dV_1(t)}{dt} = \frac{1}{C_1} \frac{dq}{dt} = \frac{1}{C_1} (I_1(t) - I(t)) \quad \text{and} \quad (5)$$

$$V_1 = -L_1 \frac{dI_1(t)}{dt}, \quad (6)$$

where q is the charge on the capacitor C_1 .

The circuit is set up to have initial conditions $V_1(t=0) = v_0$ and $I_1(t=0) = 0$. V_1 is regarded as the longitudinal wakefield and I_1 as (proportional to) the transverse wakefield of the cavity.

Multiplying Eqs. 5 and 6 by $e^{i\omega t}$, integrating from $t=0$ to $t \rightarrow \infty$, and taking the initial conditions explicitly into account, we find

$$\begin{aligned} \tilde{I}_1 &= \tilde{I} + C_1 \int_0^\infty \frac{dV}{dt} e^{i\omega t} dt = \tilde{I} - C_1 v_0 - i\omega C_1 \tilde{V}_1 \\ &= \frac{V_1}{L_1} - C_1 v_0 - i\omega C_1 \tilde{V}_1 \\ \tilde{V}_1 &= L_1 i\omega \tilde{I}_1, \end{aligned} \quad (7)$$

*Work supported by the Department of Energy grant DE-FG03-93ER40759 and contract DE-AC03-76SF00515

MASTER

DISTRIBUTION OF THIS DOCUMENT IS UNLIMITED

where $\bar{\cdot}$ symbolizes the Fourier transform. We also used the result from the previous section in writing \bar{I} as $\frac{V_1}{Z}$ on the second line of Eq. 7. Solving for \bar{V}_1 , we find

$$\bar{V}_1 = \frac{i\frac{\omega_c}{\omega_0} v_0}{\left(\frac{\omega}{\omega_0}\right)^2 + i\frac{R}{Z}\frac{\omega}{\omega_0} - 1}, \quad (8)$$

where $\omega_0 = \frac{1}{\sqrt{L_1 C_1}}$, is the natural resonant frequency of the cavity and $R = \sqrt{\frac{L_1}{C_1}}$, is the characteristic impedance of the cavity resonant mode.

The Fourier transform of the transverse wakefield (\bar{V}_\perp) is given by

$$\bar{V}_\perp = \frac{i\zeta}{\omega L} \bar{V}_1 = \frac{-\frac{\zeta}{\omega_0^2} v_0}{\left(\frac{\omega}{\omega_0}\right)^2 + i\frac{R}{Z}\frac{\omega}{\omega_0} - 1}, \quad (9)$$

where ζ is a real geometric factor (with dimension of impedance) related to the shape of the structure and not given by our model.

C. Transverse Wakefield

The transverse wakefield in the time domain

$$V_\perp(t) = \frac{1}{2\pi} \int \bar{V}_\perp e^{-i\omega t} d\omega \quad (10)$$

is obtained from the inverse Fourier transform. The integrand has two branch points from the definition of Z (Eq. 4). We choose the branch and integration contour shown in Fig. 2 [2]. The integration is naturally divided

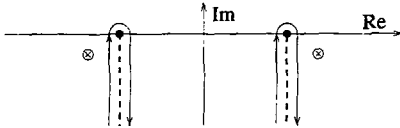


Figure 2. Contour for Calculating V_\perp

into two terms: one from the pole contribution, the other from the branch cut integral.

When $\frac{R}{Z(\omega_0)} \ll 1$, i.e. the damping term is small, the pole of the expression \bar{V}_1 is very close to ω_0 . For the purpose of calculating the pole and evaluating the residue, $Z(\omega)$ can be taken as $Z(\omega_0)$. Then the poles satisfy

$$\left(\frac{\omega}{\omega_0}\right) |_{\text{pole}} = \pm \sqrt{1 - \frac{1}{4Q^2}} - \frac{i}{2Q}, \quad (11)$$

where $Q = \frac{Z(\omega_0)}{R}$.

The branch cut integral (persistent wakefield) is evaluated with Eq. 2 and 4 in [1]. When $t' \gg 1$. The total wakefield is

$$V_\perp(t) \approx v_0 \frac{\zeta}{\omega_0 L} \left[\frac{-1}{\sqrt{1 - \frac{1}{4Q^2}}} \sin\left(\sqrt{1 - \frac{1}{4Q^2}} t'\right) e^{-\frac{t'}{2Q}} + \sqrt{\frac{2}{\pi}} \frac{\left(\frac{\omega_c}{\omega_0}\right)^{1/2}}{\left(1 - \left(\frac{\omega_c}{\omega_0}\right)^2\right)^{5/2}} \frac{1}{Q} \cos\left(\frac{\omega_c}{\omega_0} t' + \frac{1}{4}\pi\right) \frac{1}{t'^{3/2}} \right] \quad (12)$$

where $t' = \omega_0 t$.

It is clear from the above expression, that the persistent wake amplitude is proportional to $\frac{1}{Q}$, which means that a stronger damping produces a larger persistent wake. It also points out that as the resonant frequency gets closer to the waveguide cut-off, the persistent wake is enhanced.

Eq. 12 also tells us the best waveguide damping can do at a certain distance t' behind the source particle. A typical value for NLC is $t' = 40 \cdot \pi$, i.e. 20 wave lengths away.

If we ignore the oscillating factor sin, cos, the sign and take $\frac{1}{\sqrt{1 - \frac{1}{4Q^2}}} \approx 1$ in Eq. 12, it is a good approximation to regard the sum as the maxima of the oscillating amplitude of V_\perp . Thus the wakefield can be written as

$$W_\perp = W_0 \left(e^{-\frac{t'}{2Q}} + \frac{b}{Q} \frac{1}{t'^{3/2}} \right) \quad \text{with} \quad (13)$$

$$b = \sqrt{\frac{2}{\pi}} \frac{\left(\frac{\omega_c}{\omega_0}\right)^{1/2}}{\left(1 - \left(\frac{\omega_c}{\omega_0}\right)^2\right)^{5/2}}.$$

We plot b as a function of $\frac{\omega_c}{\omega_0}$ in Fig. 3.

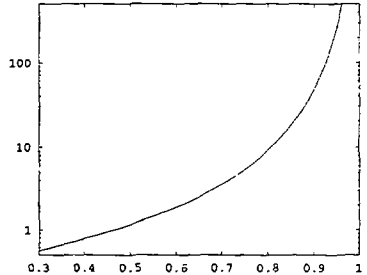


Figure 3. horizontal axis is $\frac{\omega_c}{\omega_0}$, vertical axis represents b .

At a given t' , the minimum wakefield occurs if

$$\frac{1}{2Q} = \frac{\frac{3}{2} \log t' - \log b}{t'} \quad (14)$$

i.e. decreasing Q beyond this value increases the wakefield at t' . The optimum Q as a function of t' is plotted in Fig. 4.

Substituting Eq. 14 into Eq. 13, The value of the minimum wakefield at t'

$$W_\perp^{\text{min}} = W_0 t'^{-2.5} (5b \log t' + b - 2b \log b). \quad (15)$$

is obtained. Fig. 5 displays the minimum wakefield as a function of t' for a few values of b .

III. Numerical Comparison

We have made a few MAFIA simulations on the geometry shown in Fig. 6. It is a 2-D structure with the beam passing in the Z direction. Taking the symmetry into account, only a quarter of the structure with the electric

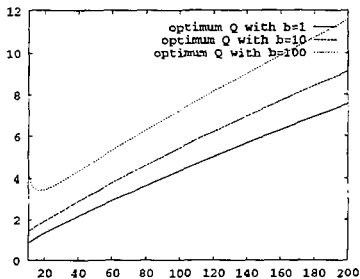


Figure 4. The three lines, from bottom to top, correspond to $b = 1, 10, 100$, respectively. The horizontal axis is $t' = \omega_c t$, and the vertical is the optimum Q value

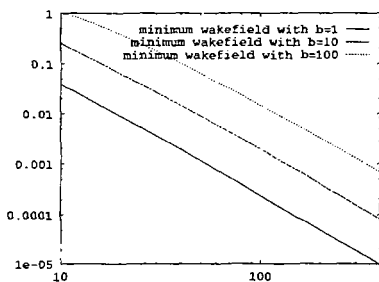


Figure 5. The three lines, from bottom to top, correspond to $b = 1, 10, 100$, respectively. The horizontal axis is $t' = \omega_c t$. The vertical axis is the minimum wakefield achieved as a ratio to the wakefield at $t' = 0$

boundary condition on the Y axis and the magnetic boundary on the X axis has been shown. We have calculated the persistent wake amplitude and the damped wake amplitude from the time domain beam excitation. The ratio of the persistent wake amplitude to the damped wake amplitude from the actual cavity waveguide system is compared with the prediction of Eq. 12 in Table I.

Four cases were run, one with $w = 0.25, t = 0.05$. The second case has $w = 0.25$ and $t = 0.25$. The third is the same as the second except that the waveguide is 1.1 times larger (other dimensions do not scale with the waveguide width.). the fourth one has the same parameters as the second except $w = 0.35$.

The circuit model and the MAFIA results agree very well considering how simple the circuit model is. The circuit model can be expected to hold only when a single decaying mode dominates the spectrum near the waveguide cutoff.

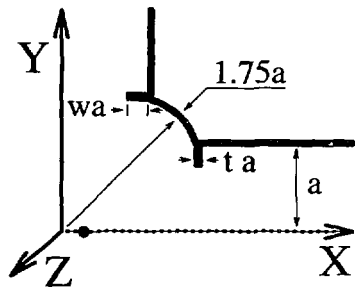


Figure 6. Waveguide damped cavity. The big dot represents the beam passing in Z direction.

| | MAFIA result | Theory | Case |
|---|--------------|--------|------|
| $Q = 3.94, \frac{\omega_c}{\omega_0} = 0.776$ | 2.17 | 2.19 | 1 |
| $Q = 6.72, \frac{\omega_c}{\omega_0} = 0.776$ | 1.17 | 1.28 | 2 |
| $Q = 7.34, \frac{\omega_c}{\omega_0} = 0.705$ | 0.587 | 0.659 | 3 |
| $Q = 12.0, \frac{\omega_c}{\omega_0} = 0.731$ | 0.251 | 0.503 | 4 |

Table I

The ratio of the persistent wake amplitude to the damped wake amplitude is compared between MAFIA simulation and the circuit model.

The discrepancy at high Q value is attributed to inadequate satisfaction of this condition.

IV. Cavity and Waveguide Detuning

For a single damped cavity, Eq. 15 presents the limit of the transverse wakefield. In the case of a multi-cell structure, the wakefield can be further reduced by detuning in analogy with dipole mode detuning.

In an optimally damped system, the dipole frequency (ω_0) and the waveguide cut-off are detuned in proportion in each cell in a Gaussian profile to produce the fastest and the most persistent fall off. In a N cell structure, detuning usually results in a wakefield which is $\frac{1}{N}$ of that of a single cell.

Taking a 100-cell structure for example, with $t' = 40\pi$ and $\frac{\omega_c}{\omega_0} = \frac{13}{15}$, the minimum wakefield of a single cell is 6.0×10^{-4} times that of an undamped cavity. With detuning, the final wakefield is down to a few parts in a million.

References

- [1] Norman M. Kroll and Xintian E. Lin, *Persistent Wakefield associated with Waveguide Damping of Higher Order Modes*, Proceedings of the 1993 IEEE Particle Accelerator Conference, Washington DC, P.3453-3455.
- [2] [1], section 2.

DISCLAIMER

This report was prepared as an account of work sponsored by an agency of the United States Government. Neither the United States Government nor any agency thereof, nor any of their employees, makes any warranty, express or implied, or assumes any legal liability or responsibility for the accuracy, completeness, or usefulness of any information, apparatus, product, or process disclosed, or represents that its use would not infringe privately owned rights. Reference herein to any specific commercial product, process, or service by trade name, trademark, manufacturer, or otherwise does not necessarily constitute or imply its endorsement, recommendation, or favoring by the United States Government or any agency thereof. The views and opinions of authors expressed herein do not necessarily state or reflect those of the United States Government or any agency thereof.